Characterization of the Early Endosome and Putative Endocytic Carrier Vesicles In Vivo and with an Assay of Vesicle Fusion In Vitro

Jean Gruenberg, Gareth Griffiths, and Kathryn E. Howell

European Molecular Biology Laboratory, 6900 Heidelberg, Federal Republic of Germany

Abstract. We have investigated two aspects of membrane traffic at early stages of endocytosis: membrane fusion and microtubule-dependent transport. As a marker, we have used the *trans*-membrane glycoprotein G of vesicular stomatitis virus implanted into the plasma membrane and then internalized for different times at 37°C. The corresponding endosomal fractions were immunoisolated using the cytoplasmic domain of the G protein as antigen. These fractions were then used in an in vitro assay to quantify the efficiency of fusion between endosomal vesicles. To identify the vesicular partners of the fusion, these in vitro studies were combined with in vivo biochemical and morphological experiments. Internalized molecules were delivered to early endosomal elements, which corresponded to a network of tubular and tubulovesicular structures. Rapid recycling back to the plasma membrane and routing to late stages of the pathway occurred from these early endosomal elements. These elements exhibited a high and specific fusion activity with each other in vitro, suggesting that individual elements of the early endosomal compartment interact with each other in vivo. After their appearance in the early endosome, the molecules destined to be degraded were observed at the next stage of the pathway in distinct spherical vesicles (0.5 μm diam) and then in late endosomes and lysosomes. When the microtubules were depolymerized with nocodazole, endocytosis proceeded as in control cells. However, internalized molecules remained in the spherical vesicles and did not appear in late endosomes or lysosomes. These spherical vesicles had relatively little fusion activity with each other or with early endosomal elements in vitro. Our observations suggest that the spherical vesicles mediate transport between the early endosome and late endosomes and that this process requires intact microtubules.

MEMBRANE proteins and solutes internalized by animal cells are delivered to the endosomal compartment before being recycled back to the cell surface or routed to the lysosomes (for reviews, see Silverstein et al., 1977; Steinman et al., 1983; Helenius et al., 1983; Pastan and Willingham, 1985; Goldstein et al., 1985; Wileman et al., 1985; and Pearse, 1987). Morphological observations, subcellular fractionation experiments, and kinetic studies of internalization, recycling, and degradation suggest that at least two populations of endosomes are involved in the transport from the cell surface to the lysosomes. Internalized molecules are first observed in early tubulovesicular endosomal elements, from which some receptors are likely to recycle rapidly back to the cell surface (Ciechanover et al., 1983; Geuze et al., 1983; Harding et al., 1983; Hopkins and Trowbridge, 1983; Oka and Weigel, 1983*b*; Mellman et al., 1984; Mueller and Hubbard, 1986; Schmid et al., 1988). Molecules destined to be degraded are then transported to late endosomes with a complex vesicular and multivesicular appearance, which are often observed in the perinuclear region, where the lysosomes are found (Wall et al., 1981; Hopkins, 1983; Wall and Hubbard, 1985; Limet et al., 1985; Baenziger and Fiete, 1986; Tran et al., 1987; Branch et al., 1987; Griffiths et al., 1988). Further evidence for a distinction between early and late endosomes is that they also differ in their acidification properties (Fuchs et al., 1989). Biochemical and functional analysis of early and late endosomes has been difficult, because of the lack of bona fide endosomal markers.

The endocytic structures responsible for the transport from the early to the late stage of the pathway have not been identified. However, the movement of endocytic vesicles between the cell periphery and the perinuclear region has been observed in vivo (Hirsch, 1962; Pastan and Willingham, 1981; Herman and Albertini, 1984) and requires microtubules (De Brabander et al., 1988). Intact microtubules are also required for the clustering of lysosomes in the nuclear region (Phaire-Washington et al., 1980; Swanson et al., 1987; Matteoni and Kreis, 1987). It is also clear that disruption of the microtubule network with drugs slows down the degradation of internalized molecules (Oka and Weigel, 1983*a*; Wolkoff et al., 1984; Berg et al., 1985; Caron et al.,

1985) without affecting the activity of lysosomal enzymes (Oka and Weigel, 1983*a*; Berg et al., 1985). The steps of the pathway from the plasma membrane to the lysosomes that require intact microtubules remain unclear.

To provide in vitro experimental systems for the study of membrane traffic in endocytosis, several investigators have recently designed cell-free assays that reconstitute some of the fusion events occurring between vesicles (Altstiel and Branton, 1983; Davey et al., 1985; Gruenberg and Howell, 1986, 1987; Braell, 1987; Diaz et al., 1988; Woodman and Warren, 1988). Using different approaches, three of these groups have compared the fusion activity in vitro at different stages of the pathway and have observed that this activity was higher at an early stage. Fusion was detected with a fusion-specific reaction using as substrate either a *trans*-membrane viral protein (Gruenberg and Howell, 1986, 1987), a fluid phase marker (Braell, 1987), or a ligand of the mannose-receptor (Diaz et al., 1988). However, the subcellular identity of the vesicular partners undergoing fusion has not yet been characterized in these assays.

In our cell-free studies, we have used endosomal fractions immunoisolated on a solid support as the acceptor component of the fusion reaction (Gruenberg and Howell, 1986). The antigen used in immunoisolation was the cytoplasmic domain of the vesicular stomatitis virus (VSV) G protein. The G protein was implanted into the plasma membrane and subsequently internalized for different times. The donor was a postnuclear supernatant (PNS)[1] prepared from cells lacking the G protein, that had internalized lactoperoxidase for 30 min at 37°C. After mixing acceptor and donor at 37°C in the presence of ATP, the occurrence of fusion was detected by a subsequent iodination of the G protein itself. The fusion-specific iodination was maximal when the acceptor was an early endosomal fraction prepared 5 min after G protein internalization. When later acceptor fractions were used, the signal decreased exponentially with the time of internalization showing a $t_{1/2} \approx 5$ min (Gruenberg and Howell, 1987).

In this paper, we have continued to characterize the traffic of membrane in endocytosis. Our cell-free assay using endosomal fractions was modified by introducing a detection system similar to that developed by Braell (1987). The occurrence of fusion was monitored by the formation of a fusion-specific complex between avidin and biotinylated horseradish peroxidase. These in vitro observations were correlated with in vivo studies in the presence and in the absence of intact microtubules, thus enabling us to identify (*a*) the vesicular partners undergoing fusion (acceptor and donor) and (*b*) putative endocytic carrier vesicles that depend on intact microtubules.

Materials and Methods

Cells and Viruses

Monolayers of baby hamster kidney (BHK-21) cells were grown in G-MEM supplemented with 5% FCS, 10% tryptose phosphate broth, and 2 mM glutamine. The cells were always seeded at a density of $4 \times 10^4/cm^2$ of culture dish from a stock that was allowed to grow to confluency for 3 d and were used 14 h after passage. This protocol guaranteed a very homogenous population of cells that produced an optimal homogenate for subsequent immunoisolation. Manipulations of the cells were always at ice temperature, except when indicated. VSV and [^{35}S]methionine-labeled VSV were grown and harvested as described (Gruenberg and Howell, 1985, 1986).

To investigate the role of microtubules in endocytosis, the conditions of microtubule depolymerization in BHK cells were first defined. As judged by fluorescence microscopy with antitubulin antibodies, it was necessary to preincubate the cells for 150 min at 37°C with 10 μM nocodazole to depolymerize the microtubules (not shown). Then, the G protein was implanted into the plasma membrane and internalized at 37°C, as described below, in the presence of 10 μM nocodazole in all the solutions up to the internalization step.

Immunological Reagents

The polyclonal antibody against avidin was obtained from Calbiochem-Behring Corp., La Jolla, CA. We raised the polyclonal antibody against horseradish peroxidase (HRP) in rabbits using HRP from Sigma Chemical Co. (St. Louis, MO) as antigen and the polyclonal antibody against G protein using a micellar preparation of the G protein as antigen. The mAb against an exoplasmic epitope of the G protein was a gift of K. Simons (European Molecular Biology Laboratory; clone 17.2.21.4). For time-resolved fluorescence, the following reagents were labeled with Europium (Eu) by I. Hemmilä (Wallac Oy, Turku, Finland): the affinity-purified antibodies raised in sheep against the Fc portion of mouse IgG or rabbit IgG, protein A (Pharmacia Fine Chemicals, Piscataway, NJ) and avidin (Calbiochem-Behring Corp.). The solid supports used in immunoisolation experiments were either polyacrylamide beads (Bio-Rad Laboratories, Richmond, CA) or monodisperse magnetic beads (Ugelstad et al., 1983; Howell et al., 1988*a*,*b*) with a covalently coupled linker antibody against the Fc portion of mouse IgG. The immunoadsorbent was prepared by binding the mAb against a cytoplasmic epitope of the G protein (clone P5D4; Kreis, 1986) to the solid support as described (Gruenberg and Howell, 1985; Howell et al., 1989).

Cell-free Assay of Vesicle Fusion Using Immunoisolated Endosomal Fractions

The cell-free assay was carried out by mixing an acceptor fraction, immunoisolated via the G protein on a solid support, with a donor fraction, a PNS prepared from cells lacking the G protein. The number of cells used to prepare the donor and the acceptor fractions for each experiment was always identical.

Acceptor. We have previously described our approach using immunoisolated endosomal fractions as acceptor in cell-free fusion studies (Gruenberg and Howell, 1986, 1987). Briefly, the G protein was implanted in the plasma membrane by low pH mediated fusion of the viral envelope with the plasma membrane (White et al., 1980; Gruenberg and Howell, 1985). In all experiments, 41 μg VSV were added to 1.3×10^7 cells in a 75-cm^2 Petri dish; 8 μg total VSV protein were fused with the plasma membrane, corresponding to a density of 70 G molecules/μm^2 membrane surface area. The G protein remained restricted to the plasma membrane because the cells were kept at ice temperature. When the cells were warmed up to 37°C, the G protein was rapidly internalized as a single and synchronous wave. In a typical experiment, two 75-cm^2 Petri dishes were used for each incubation time.

Internalization was carried out in the presence of 1.7 mg/ml avidin in MEM buffered to 7.4 with 10 mM Hepes, containing 10 mM D-glucose and prewarmed to 37°C. At the desired time the cells were returned to ice temperature, washed 3 times for 5 min each with PBS containing 5 mg/ml BSA (PBS-BSA) and scraped with a rubber policeman. The cells were centrifuged at 100 *g* for 5 min, the pellet was resuspended in 5 ml homogenization buffer (250 mM sucrose buffered to pH 7.4 with 10 mM Tris-HCl) and centrifuged again at 100 *g* for 5 min. The pellet was then resuspended in 0.5 ml of homogenization buffer and passed 10 times through the tip of a 1-ml Pipetman (Gilson Co., Inc., Worthington, OH). The homogenate was then centrifuged at 1,000 *g* for 10 min and the PNS was removed. The PNS was diluted with 1 ml PBS-BSA and recentrifuged at 1,000 *g* for 15 min. This supernatant was the input for the immunoisolation experiments. Immunoisolation was carried out for 2 h at 4°C using 1 mg of immunoadsorbent and 500 μg of PNS protein in a final volume adjusted to 1 ml with PBS-BSA. Then, the immunoadsorbent plus bound vesicles was retrieved as described (Gruenberg and Howell, 1986; Howell et al., 1989), resuspended in 100 μl homogenization buffer and immediately used in the cell-free assay.

Donor. Cells without implanted G protein were washed twice with PBS. The cells were released from the dish using 1 ml trypsin-EDTA (Gibco

1. *Abbreviations used in this paper*: biotHRP, biotinylated horseradish peroxidase; HRP, horseradish peroxidase; PNS, postnuclear supernatant.

Laboratories, Grand Island, NY) for one 75-cm^2 Petri dish for 3 min at room temperature. Then 2 ml PBS-BSA containing 0.1 mg/ml soybean trypsin inhibitor were added and the cells were centrifuged for 5 min at 100 *g*. The cell pellet was resuspended in PBS-BSA and washed three times by centrifugation. Then, the cell pellet was resuspended in 1 ml PBS containing 10 mM D-glucose, 10 mM Hepes and 1.7 mg/ml biotinylated HRP (biotHRP) prewarmed to 37°C and incubated for the indicated time at 37°C. After incubation, the cells were cooled to ice temperature, diluted 10 times with ice-cold PBS-BSA, centrifuged and washed three times as described above. In pulse-chase experiments, the cells were reincubated at 37°C for the indicated times in 5 ml of MEM buffered to 7.4 with 10 mM Hepes, containing 10 mM D-glucose, 0.2% BSA and prewarmed to 37°C, and then cooled on ice, diluted with 4 vol of PBS-BSA and centrifuged. After the washes, the cell pellet was resuspended in 0.5 ml homogenization buffer and the cells were passed 10 times through an 8.02-mm precision bore in a metal block containing an 8.002 metal ball-bearing (Balch et al., 1984). The homogenate was centrifuged for 10 min at 1,000 *g* and the PNS was used as donor in the cell-free assay. In a typical experiment, six dishes were used to prepare one donor PNS.

Cell-free Assay. The different components of the assay were rapidly mixed on ice in the following order: (*a*) 24 μl of a mixture containing 125 mM Hepes-KOH (pH 7.0), 0.5 M KCl, 15 mM $Mg(OAc)_2$ and 10 mM DTT; (*b*) 5.2 μl of 0.5 mg/ml biotinylated insulin (Sigma Chemical Co.); (*c*) 10 μl of an ATP-regenerating system, prepared freshly by mixing 1:1:1 vol of stock solutions of 100 mM ATP, 800 mM creatine phosphate, and 4 mg/ml creatine phosphokinase at 800 U/ml (Boehringer Mannheim, FRG); (*d*) the acceptor in 100 μl homogenization buffer; (*e*) 100 μl of the donor PNS. When the assay was carried out in the absence of ATP, the ATP-regenerating system was omitted and replaced by 8 μl of an ATP-depleting system, freshly prepared with 0.5 mg hexokinase (1,400 U/ml; Boehringer Mannheim) in 50 μl of 250 mM D-glucose. The mixture was allowed to stay on ice for an additional 2 min, and was then warmed to 37°C and incubated for the time indicated. After the assay, the mixture was first cooled to ice temperature and then diluted with 1 ml ice-cold PBS-BSA. The beads plus bound material were retrieved and resuspended in 50 μl ice-cold PBS-BSA. Before solubilization, 5 μl of biotinylated insulin was added. When the amount of avidin in the acceptor was quantitated, biotinylated insulin (10 μl at 0.5 mg/ml) was present only during immunoisolation and was replaced before solubilization with 10 μl of 0.18 mg/ml biotHRP. The bound material was then solubilized on ice for 15 min after adding 5 μl of a mixture of 10% Triton X-100 and 0.5% SDS. The samples were then diluted with 450 μl of PBS-BSA, the beads were removed by centrifugation in a microfuge (Beckman Instruments, Inc., Fullerton, CA) and 200 μl duplicates of the supernatant were analyzed for the enzymatic activity of the avidin-biotHRP complex with an ELISA.

Detection System. The avidin-biotHRP complex was quantitated using an ELISA. Microtiter wells were coated overnight at 4°C with 2 μg of affinity-purified antiavidin antibody in 0.1 M $NaHCO_3/Na_2CO_3$ (pH 9.0) per well. The plates were washed with PBS, quenched for 1 h at room temperature with PBS-BSA, and washed twice with PBS-BSA. The reaction mixture containing the avidin-biotHRP complex was added and incubated for 2 h at room temperature. The plates were washed six times with PBS-BSA containing 0.1% Tween-20 and the enzymatic activity of the bound HRP was determined (see below).

Quantitation of G Protein on the Cell Surface with a Time-resolved Immunofluorometric Assay

The G protein was implanted into the plasma membrane as described above. Internalization was carried out in MEM, 10 mM Hepes (pH 7.4) containing 0.2% BSA and 10 mM D-glucose for the indicated times. The cells were returned to ice temperature and washed twice with PBS. The cells were then incubated for 30 min on ice with 7.4-MEM (MEM, 10 mM *N*-tris[hydroxymethyl]methyl-2-aminoethane sulfonic acid [Tes], 10 mM Mops, 15 mM Hepes, 2 mM NaH_2PO_4, and 350 mg/liter $NaHCO_3$, pH 7.4) containing 20 mM *N*-acetylglucosamine, 5 mg/ml BSA, and the mAb against G exoplasmic domain at 1 μg/ml. The antibody was removed and the monolayers were washed three times for 5 min each with PBS-BSA. The amount of bound antibody was determined by adding 200 ng of an anti-mouse Fc antibody labeled with Eu in 2.5 ml PBS-BSA for one 75-cm^2 dish. After 1 h on ice, the excess detecting antibody was removed and the cells were washed three times for 5 min each with PBS-BSA. The bound Eu was released with 500 μl Enhancer solution (Wallac Oy) for 30 min on ice. The Enhancer solution was collected and counted in 200-μl aliquots in duplicate in an ARCUS/DELFIA time-resolved fluorometer (Wallac Oy).

When the G protein was cross-linked with antibodies on the cell surface, the protocol remained the same except that the polyclonal antiserum against G protein was used at a dilution of 1:200 in 7.4-MEM-BSA containing 20 mM *N*-acetylglucosamine and reacted with the cells for 30 min on ice before the internalization step. The cells were washed three times for 5 min each with PBS-BSA and the G protein/antibody complex was internalized. The amount of antibody on the cell surface was detected with 200 ng Eu-labeled protein A as above.

Quantitation of G Protein Degradation

All protocols for implantation/internalization were identical except that 5 × 10^6 dpm of ^{35}S-labeled VSV were added per 75-cm^2 Petri dish. At the end of internalization, the cells were scraped in PBS, centrifuged at 100 *g* for 5 min and resuspended in 10 mM Tris (pH 7.4), containing 1 mM PMSF, 1 mM iodoacetamide, 10 μg/ml aprotinin, 1 μg/ml pepstatin, 17 μg/ml benzamidine, and 1 μg/ml antipain. After 5 min to allow swelling of the cells to occur, the cells were homogenized by repeated pipetting, centrifuged at 1,000 *g* for 10 min and the supernatant was collected. Then, the G protein was extracted in Triton X-114 (Bordier, 1981). Proteins in both the detergent and the water phases were precipitated in 90% acetone at −20°C and analyzed by SDS-PAGE using the buffer system of Maizel (1971). The labeled viral proteins were revealed by autoradiography and quantitated by densitometric scanning using a Quick Scan R & D densitometer (Helena Laboratories, Beaumont, TX).

Electron Microscopy

The G protein was labeled on the cell surface before internalization with the polyclonal antibody as described above. The cells were then washed three times for 5 min each in PBS-BSA and reacted with protein A-colloidal gold (Au-13 nm) in 7.4-MEM-BSA for 45 min at ice temperature. The G protein/Au complexes were then internalized for the indicated times with or without HRP at 5 mg/ml in the same buffer as above. The cells were then washed twice in PBS and fixed in 1% glutaraldehyde in 200 mM cacodylate buffer, pH 7.4. They were subsequently treated with osmium tetroxid and embedded in Epon. Acid phosphatase cytochemistry was carried out as described by Griffiths et al. (1983*a*) and internalized HRP was visualized as described by Marsh et al. (1986).

For the quantitation of the gold particles in the acid phosphatase-positive compartments, 25 micrographs were taken at random at a primary magnification of 6,000. Each structure containing the reaction product of acid phosphatase was also photographed at a magnification of 25,000, to clearly visualize the gold particles. The volume density of the acid phosphatase-positive structures was determined by point counting methods (Weibel, 1979; Griffiths and Hoppeler, 1986).

For microscopic examination of the immunoisolated fractions, the same protocol for G implantation, gold labeling, and internalization was used. The cells were homogenized, a PNS was prepared, and the fractions were immunoisolated from the PNS. Then the fractions were embedded in 1% low melting agarose in 200 mM Hepes (pH 7.4) buffer and fixed for 30 min in 1% paraformaldehyde in 200 mM Hepes (pH 7.0). After washing in the Hepes buffer, the fractions were frozen and processed as described by Griffiths et al. (1983*b*).

Analytical Techniques

Biotinylation of HRP. 20 mg HRP in 9.5 ml of 0.1 M $NaHCO_3/Na_2CO_3$ (pH 9.0) was mixed with 11.4 mg of biotin-X-NHS (Calbiochem-Behring Corp.) in 0.5 ml dimethylformamide for 2 h at room temperature. This corresponds to a 50:1 molar excess of biotin over HRP. The unreacted active groups were quenched with 1 ml of 0.2 M glycine (pH 8.0) and mixed for an additional 30 min. The mixture was dialyzed against several changes of PBS. The final biotHRP, 1.8 mg/ml, exhibited the same specific enzymatic activity as native HRP (not shown). Time-resolved fluorescence was used to monitor the extent of biotinylation. Serial dilutions of biotHRP were adsorbed directly onto the plastic of microtiter wells overnight in PBS. Detection was either with a polyclonal antibody against HRP itself followed by Eu-labeled sheep anti-rabbit Fc antibody or directly with Eu-labeled avidin. Titration of biotHRP was compared with native HRP with the anti-HRP antibody. These data demonstrated that all molecules of HRP were biotinylated (not shown).

HRP Enzymatic Activity. The HRP enzymatic activity in cell extracts or in microtiter wells was measured at 460 nm using 0.342 mM *o*-dianisidine and 0.003% H_2O_2 as substrates in 0.5 M Na-phosphate buffer pH 5.0 containing 0.3% Triton X-100.

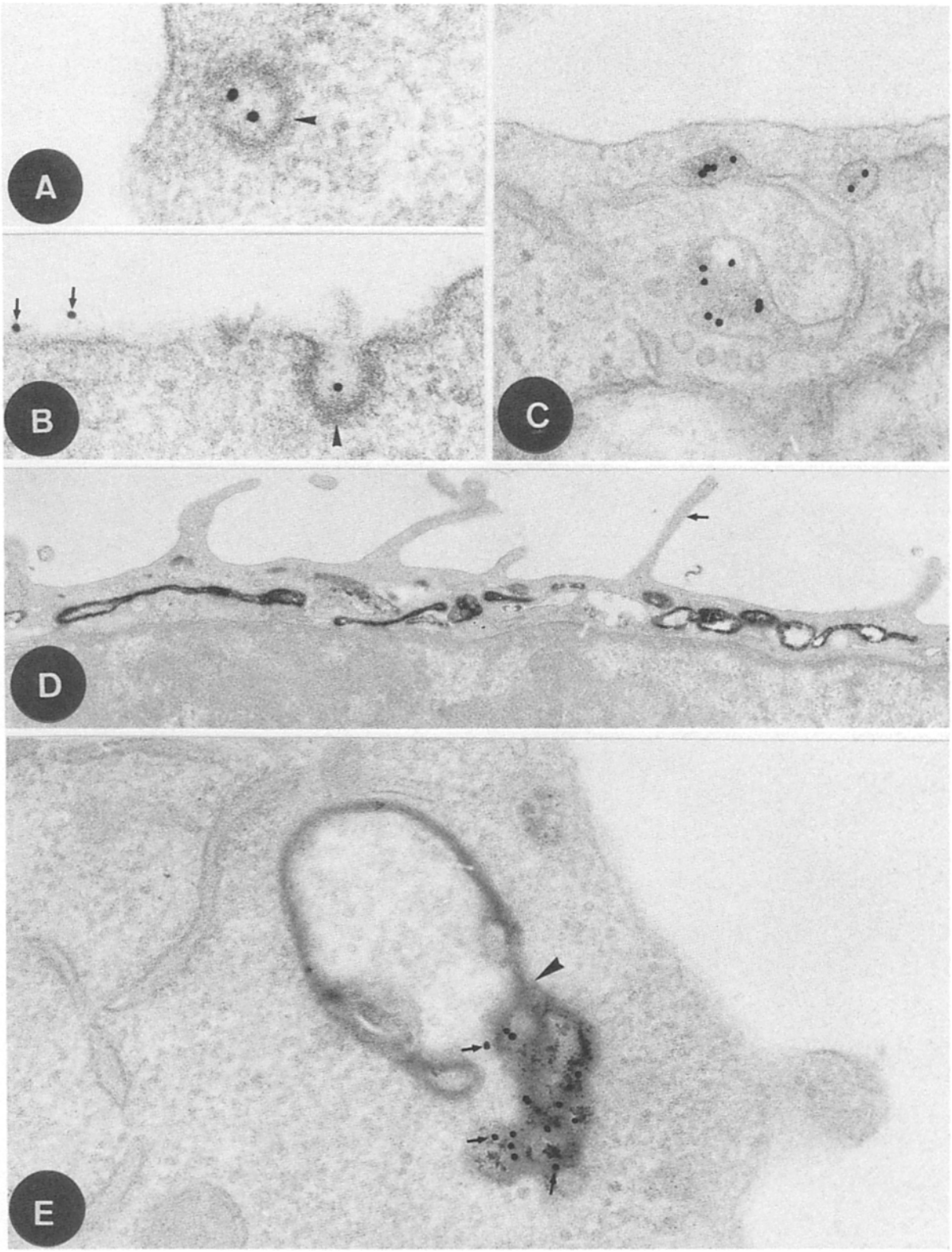

Figure 1. G protein distribution in early endosomal elements in the presence and in the absence of microtubules. After implantation into the plasma membrane, the G protein was labeled with the polyclonal antibody followed by protein A-gold (13 nm). The cells were incubated for 5 min at 37°C in the presence (*C* and *D*) or in the absence (*A*, *B*, and *E*) of 10 μM nocodazole to depolymerize the microtubules and were then fixed and processed for electron microscopy. (*A* and *B*) Gold particles were internalized via coated pits (*B*) and coated vesicles (*A*). Arrowheads in *A* and *B* point at the clathrin coat, whereas the arrows in *A* point at gold particles on the plasma membrane. (*C–E*) The gold particles were observed in early, tubulovesicular endosomal elements. These elements exhibited the same morphology after microtubule depolymerization (*C* and *D*) and in control cells (*E*). In *D* and *E*, these elements were also visualized by the reaction product of HRP, after cointernalization of HRP and G protein. In *D*, the arrow points a microvillus on the cell surface. In *E*, the arrowhead points at the neck of a connection between the tubular-reticular and the vesicular parts of the endosome and the arrows indicate the gold particles. *A* and *B*, ×120,000; *C*, ×93,000; *D*, ×17,000; *E*, ×91,000.

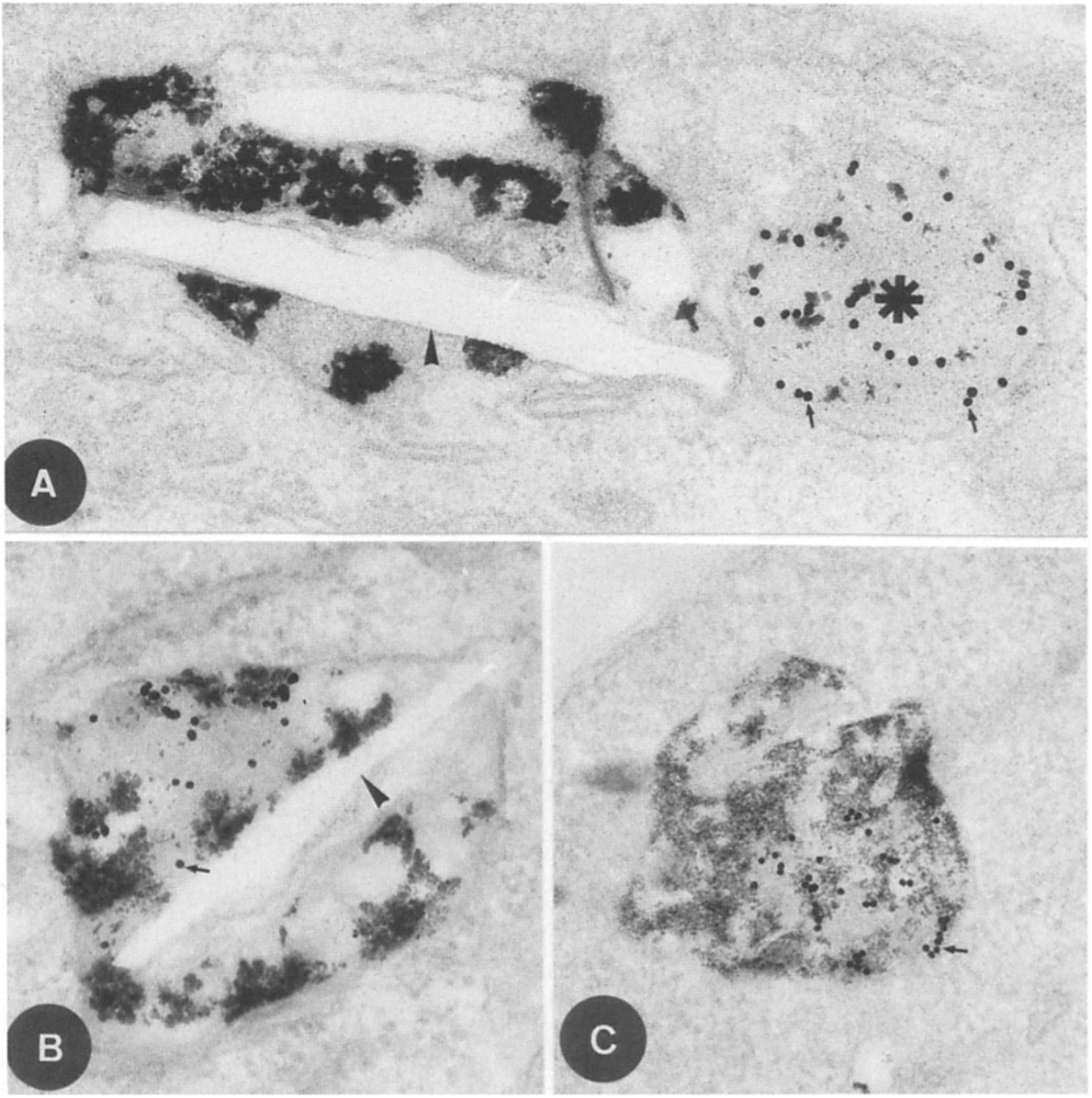

Figure 2. G protein distribution in acid phosphatase-positive prelysosomes or lysosomes in the presence of microtubules. The experimental conditions were as shown in Fig. 1, in the absence of nocodazole. Lysosomes (and possibly late endosomes/prelysosomes; see Discussion) were revealed by acid phosphatase cytochemistry. (*A*) The G protein/gold complexes were internalized for 15 min at 37°C. A large vesicle (*asterisk*) containing gold particles (*arrow*) is seen next to an acid phosphatase-positive structure. (*B* and *C*) After 45 min internalization, the gold particles (*arrows*) have moved to acid phosphatase-positive elements. Acid phosphatase-positive vesicles with a complex morphology often contain long rod-like structures (*A* and *B*; *arrowhead*) and may represent prelysosomes (see Discussion). *A*, ×110,000; *B*, ×95,000; *C*, ×88,000.

Protein Determination. The protein was determined according to Bradford (1976).

Results

Morphology of the Endosomal Elements

The endosomal elements containing the G protein after different times of internalization were identified by electron microscopy. The G molecules were implanted into the plasma membrane and labeled with a polyclonal antibody followed by protein A-colloidal gold. These experimental steps were carried out at ice temperature to restrict the labeled G molecules to the cell surface. Then, the G protein/gold complexes were internalized for different times at 37°C. Cross-linking of the G molecules with antibodies prevents recycling and guarantees that all the G molecules are transported towards the lysosomes as a single and synchronous wave (Gruenberg and Howell, 1987; see Figs. 4 and 5).

The G protein/gold complexes were internalized via coated pits and vesicles (Fig. 1, *A* and *B*) and after 5 min were localized in a reticulum of tubular, cisternal, and tubulovesicular elements. The morphology of these early endosomal elements could be better visualized by labeling their content using HRP cointernalized with the G protein/gold complexes (Fig. 1 *E*; see also the overview in Fig. 1 *D* after microtubule depolymerization). Between 5 and 15 min internalization, the G molecules were observed also in large spherical vesicles with a diameter ranging from 0.4 to 0.7 μm (Fig. 2 *A*).

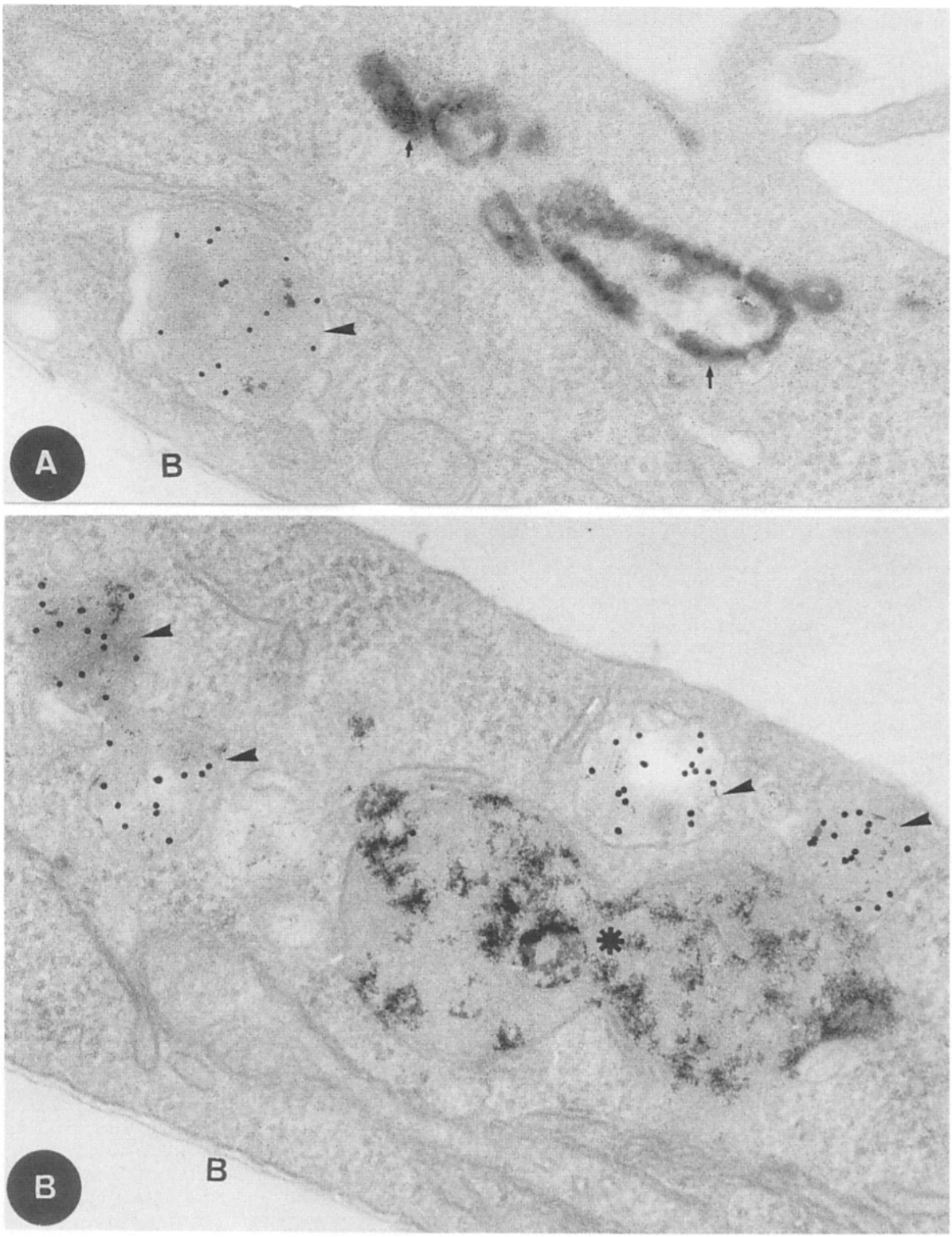

Figure 3. G protein distribution in the spherical vesicles in the absence of microtubules. The experimental conditions were as in Figs. 1 and 2; internalization was for 45 min in the presence of 10 μM nocodazole. (*A*) The G protein/gold complexes were internalized for 40 min without HRP and then for an additional 5 min in medium containing 5 mg/ml HRP. Early tubulovesicular endosomal elements that contain the reaction product of HRP (*arrow*) are distinct from a large HRP-negative spherical vesicle (*arrowhead*), where the gold particles have accumulated. (*B*) A lysosome (or a prelysosome) is revealed by acid phosphatase cytochemistry (*asterisk*). The gold particles were not seen in the acid phosphatase–positive structure, but accumulated in large spherical vesicles (0.4–0.7 μm; *arrowhead*), similar to the vesicles seen after 15 min internalization in the absence of nocodazole (Fig. 2 *A*). The basal side of the cell, facing the plastic of the culture dish is indicated in both *A* and *B*. *A*, ×79,000; *B*, ×87,000.

Table I. Morphometric Analysis of the Subcellular Distribution of the G Protein with and without Intact Microtubules

G protein internalization	No nocodazole	10 μM nocodazole
	gold particles/μm² of vesicular profile	
25 min + 5-min pulse of HRP		
HRP⁺, tubulo-vesicular elements	29.4 ± 8.0	29.4 ± 8.4
HRP⁻ and AcPase⁻, spherical vesicles	186.0 ± 63.0	138.0 ± 54.0
45 min		
AcPase⁺, lysosomes (prelysosomes)	16.5 ± 5*	0.7 ± 0.3*

* The volume density of acid phosphatase-positive (AcPase⁺) compartments remained similar after nocodazole treatment (2.49 ± 0.6% of the cytoplasmic volume) when compared with control cells (2.14 ± 0.5%).

In these experiments, the late endosomes and the lysosomes were visualized by acid phosphatase cytochemistry. Although acid phosphatase has always been considered a marker of the lysosomes, recent data indicate that late endosomes are also reactive (Griffiths, G., R. Matteoni, R. Back, and B. Hoflack, manuscript in preparation), in agreement with earlier observations of Storrie et al. (1984). In this study, we will refer to the acid phosphatase-positive, late endosomes as prelysosomes. The G protein/gold complexes were observed in the large spherical vesicles before being seen in prelysosomes or lysosomes. After 45 min internalization, the bulk of the gold particles had reached acid phosphatase-positive elements (Fig. 2, *B* and *C*).

Large Spherical Vesicles

Several morphologically distinct structures or compartments could be identified during G protein endocytosis: the plasma membrane, coated pits and vesicles, tubulovesicular elements, large spherical vesicles, and acid phosphatase-positive prelysosomes and lysosomes (Figs. 1 and 2). If intact microtubules are required for any transport step between these morphologically distinct compartments, their depolymerization would be expected to prevent delivery to more distal compartments. The effect of microtubule depolymerization on the subcellular distribution of the internalized G molecules was therefore investigated. To promote microtubule depolymerization, the cells had to be preincubated with 10 μM nocodazole for 150 min at 37°C (not shown) and nocodazole was present in all solutions during the experiment. The G protein was then implanted, labeled with colloidal gold, and internalized at 37°C.

After 5 min internalization, the G protein/gold complexes were cleared from the cell surface and internalized into endosomal elements (Fig. 1, *C* and *D*) that were morphologically indistinguishable from the elements observed in control cells (Fig. 1 *E*). The high magnification micrograph (Fig. 1 *C*) should be compared with the control (Fig. 1 *E*). An overview of the early endosome visualized with the reaction product of HRP co-internalized with the G protein is shown in Fig. 1 *D*. Unlike tubular lysosomes (Swanson et al., 1987), the early endosomal elements clearly retained their tubular and tubulovesicular morphology after microtubule depolymerization.

After longer incubations in the presence of nocodazole, the G molecules were observed in large spherical vesicles of 0.4–0.7 μm diameter (Fig. 3). These vesicles appeared identical to the vesicles observed in the control cells after 5–15 min internalization (Fig. 2 *A*). However, in contrast to the observations made in control cells, the G molecules remained in these spherical vesicles during longer incubations. Even after 45 min, the appearance of G protein in acid phosphatase-positive prelysosomes and lysosomes was significantly reduced (Fig. 3 *B*, see Table I). We took advantage of this effect of microtubule depolymerization to determine whether the spherical structures are elements of the tubulovesicular network of the early endosome. For this experiment, the early endosomal elements were labeled with a 5-min pulse of HRP after G protein had been already internalized for 25 min. The HRP during the 5-min pulse did not reach the spherical vesicles in which the G protein/gold complexes had accumulated (Fig. 3 *A*), showing that these vesicles are structurally distinct from the early endosome.

Morphometric Analysis of the Subcellular Distribution of G Protein in the Presence and Absence of Microtubules

In the absence of microtubules, the amount of G protein/gold complexes observed in the early endosome decreased, yet the complexes did not reach acid phosphatase-positive elements (Fig. 3). To characterize these observations in more detail, a morphometric analysis was carried out (Table I). First, the decrease of G molecules in the early endosome and their appearance in the spherical vesicles were quantitated after 30 min internalization in the presence and absence of microtubules, using the same protocol as that used in Fig. 3 *A*. The tubulovesicular endosomal structures were scored morphologically with the reaction product of HRP after a pulse of 5 min, after a 25-min internalization of the G protein. The large, spherical vesicles containing gold particles were scored according to both their typical morphology and the absence of reaction product for both HRP (early endosome) and acid phosphatase (prelysosomes and lysosomes). In these spherical vesicles, the density of gold particles/μm² of vesicular profile was similar both in the presence of microtubules (186 ± 63) or in their absence (138 ± 54). This shows that the number of G molecules packaged in the vesicles was the same under both conditions. The density of gold particles remaining in the HRP-positive early endosome after 30 min internalization was approximately five times lower than in the spherical vesicles in both cases. This demonstrates that microtubule depolymerization did not impair the step of the pathway between the early endosome and the spherical vesicles.

Next, the distribution of G protein/gold complexes in acid phosphatase-positive structures after 45 min internalization was quantified (Table I). This analysis was restricted to structures containing significant amounts of reaction product: early endosomes often contain small deposits of reaction product, whose significance is not clear. In the presence of microtubules, the density of gold particles in acid phosphatase-positive structures was 16 ± 5 gold particles/μm² of vesicular profile. This density was only ≈10% of that observed in the spherical vesicles. This is likely to reflect a higher concentration of G molecules in the vesicles and their subsequent dilution in the larger total surface area and vol-

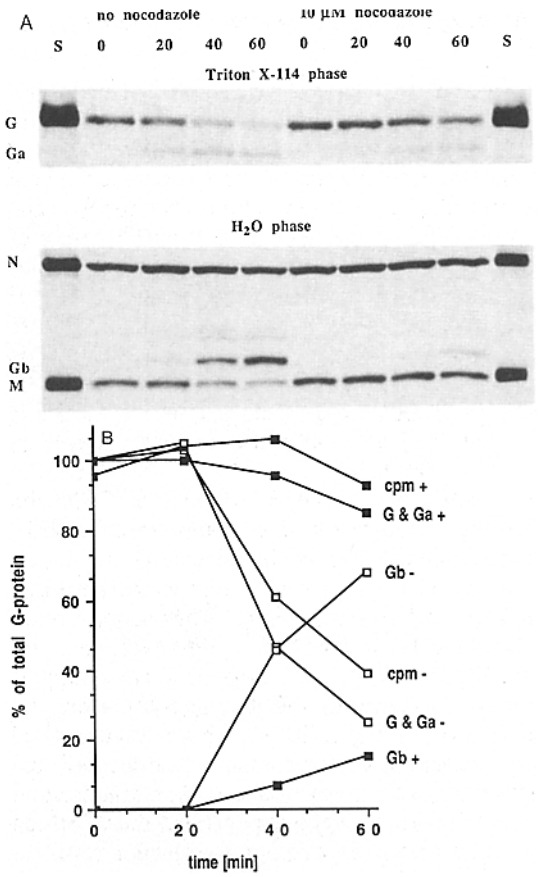

Figure 4. G protein degradation. The amount of G protein degraded was quantitated using ^{35}S-labeled VSV. (*A*) The implanted G molecules were cross-linked with a polyclonal antibody and subsequently internalized for the indicated times with or without 10 μM nocodazole. Then, the membrane-spanning forms of the [^{35}S]G protein were extracted in Triton X-114. Both the detergent and the water (H_2O) phases were analyzed by gel electrophoresis and autoradiography. The G protein (67 kD) was processed during the incubation first into G_a (≈60 kD), a membrane-spanning form, and later into the water soluble G_b (≈28 kD). The other viral proteins partition in the water phase (N, 50 kD; M, 24 kD). (*B*) The detergent phases were directly counted (indicated as *cpm*) and the values are compared with the densitometric values obtained from the bands in *A*, corresponding, respectively, to the sum of G and G_a (G + Ga) or G_b. *Open symbols*, without nocodazole; *solid symbols*, with nocodazole.

ume of the acid phosphatase–positive structures. In the absence of microtubules, the density of gold particles in acid phosphatase–positive structures dropped from 16 ± 5 to 0.7 ± 0.3 gold particles/μm^2 of vesicular profile. These data show that in the absence of microtubules, the G molecules remain in the spherical vesicles and do not appear in acid phosphatase–positive prelysosomes or lysosomes.

G Protein Degradation

The effect of microtubule depolymerization on the transport of the internalized G molecules to a degradative compartment was directly quantified. Conditions were similar to those used for the morphological analysis (Figs. 1–3). VSV metabolically labeled with [^{35}S]methionine was used for the implantation of the G protein in the plasma membrane. The cells were then incubated at 37°C for increasing times and extracted with Triton X-114. All viral proteins are labeled, but only the membrane-spanning G protein partitions into the detergent phase. Both the detergent and the water phases were analyzed by gel electrophoresis and autoradiography (Fig. 4 *A*). Degradation of the G protein was quantified by densitometric scanning of the gel and compared with the direct counting of the detergent phases (Fig. 4 *B*). The water phase contains the other viral proteins (M and N), which account for ≈78% of the total [^{35}S]methionine of the virus.

In the absence of nocodazole, a fraction of the G protein (67 kD) was processed within 20 min to a smaller form (G_a ≈ 60 kD). G_a also partitioned into the detergent phase, and presumably retained its membrane-spanning domain (Fig. 4 *A*). A second processed form of the G protein (G_b ≈ 28 kD) appeared in the water phase. After 60 min, ≈70% of the G protein was processed (Fig. 4 *B*) and the label was recovered in G_b. This indicated that G_b originated from the cleavage of G (or G_a) into soluble peptides of equal mobility; sequence analysis has shown that methionine residues are equally distributed throughout the G protein (Rose and Gallione, 1981). When the G protein was not cross-linked with an antibody before internalization, the fraction of the G protein that was internalized was also cleaved to G_a and G_b with the same kinetics and to the same extent. After 60 min, 70% of the internalized, non–cross-linked G molecules were processed to G_b (not shown).

In the presence of nocodazole, this time-dependent processing of the G protein was significantly reduced. After 60 min, the G protein, together with the membrane-spanning cleaved product G_a, accounted for ≈92% of the G protein initially present. The appearance of G_b was reduced to ≈12% (Fig. 4, *A* and *B*). The depolymerization of microtubules thus resulted in a ≈ sevenfold decrease in the processing of the G protein to the 28-kD peptide after 60 min.

G Protein Endocytosis and Recycling Monitored with an Immunofluorometric Assay Using Europium

The depolymerization of microtubules reduced the delivery of G protein to a degradative compartment, as quantified both by the morphometric analysis (Table I) and by the degradation of the G protein (Fig. 4). The next step was to determine the kinetics of G protein internalization and recycling in the absence of antibody cross-linking after microtubule depolymerization. The amount of G protein at the cell surface was quantified using a new immunofluorometric assay. This technique, used for clinical immunoassays (Soini and Hemmilä, 1979; Soini and Kojola, 1983; Hemmilä et al., 1984), was applied here for the detection of cell surface antigens. The G molecules at the cell surface were labeled after various times of internalization with a mAb against the G exoplasmic domain followed by a detecting antibody, which recognized the Fc domain of mouse IgG and was labeled with Europium. Because the Eu atoms exhibit a delayed fluorescence, the emitted fluorescence can be counted in a time-resolved fluorometer as single photon events (Eu counts) after repeated pulses of excitation by light. This technique provides a higher sensitivity, lower background, and a wider dynamic range than other labels.

The depolymerization of microtubules had no effect on the kinetics of G protein internalization or recycling, as shown in Fig. 5 *A*. Both in the presence and in the absence of intact microtubules, ≈60% of the G molecules were internalized

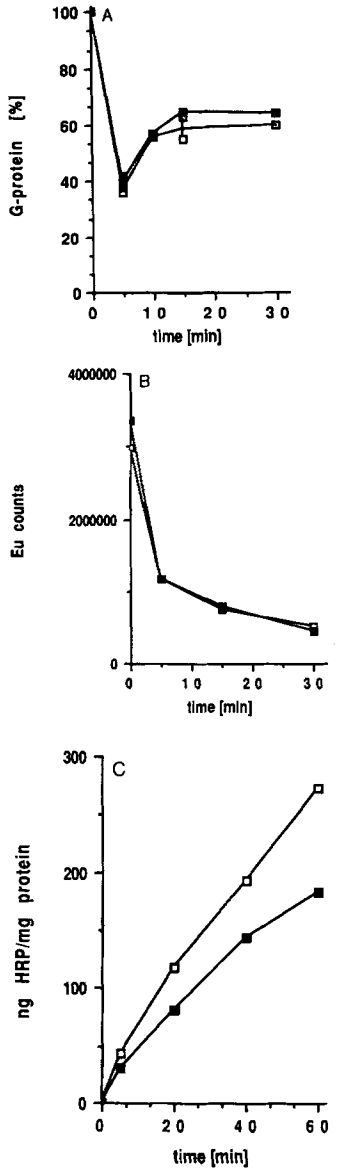

Figure 5. G protein endocytosis. The amount of G protein on the cell surface was quantitated after different times of internalization with (■) or without (□) 10 μM nocodazole using a time-resolved immunofluorimetric assay. (*A*) In the absence of antibody cross-linking, the G protein recycles to the cell surface. Different experiments have been plotted; the values are expressed as percentage of the amounts initially present on the cell surface (t = 0 min). (*B*) Recycling is abolished by antibody cross-linking. The absolute amounts of the delayed fluorescence are expressed as Eu counts (see text). The background was measured without implanted G protein or with a control antibody and was 2,552 ± 200 Eu counts. (*C*) Cells were incubated for the indicated times in the presence of HRP to provide a marker of the endosomal content (■, with 10 μM nocodazole; □, without). The amount of HRP internalized is expressed in nanograms per milligram cellular protein.

after 5 min and ≈50% of the internalized molecules recycled back to the cell surface with a $t_{1/2} \approx 5$ min. Localization of the G protein after 5 min (Fig. 1) showed that this early compartment from where recycling occurred corresponded to the tubulovesicular endosome.

In the experiments described in Figs. 1–4, the G molecules were cross-linked with an antibody before internalization. Under these conditions, recycling was abolished (Fig. 5 *B*) and all the G molecules were transported to a degradative compartment with the same kinetics as the internalized, non–cross-linked G protein (see above). Internalization of the cross-linked G molecules also was not affected by nocodazole (Fig. 5 *B*).

Nocodazole did not affect the internalization or recycling of the membrane-spanning G protein. The effect of microtubule depolymerization on the kinetics of fluid phase endocytosis was then studied using HRP as a general marker (Fig. 5 *C*). After depolymerization, HRP continued to accumulate to ≈75% of the control amount within 60 min.

Cell-free Assay of Fusion Using Immunoisolated Fractions

The experiments described above have shown that endocytosis proceeds in at least two stages: (*a*) the microtubule-independent internalization into, and recycling from, the early endosome and (*b*) the subsequent microtubule-dependent transport towards the late endosomes (or prelysosomes). The morphological analysis suggested that this transport involves spherical vesicles, which are distinct from the early tubulovesicular endosome. To provide an additional functional characterization of this pathway, we combined subcellular fractionation with a quantitative assay to measure the fusion of endocytic vesicles in vitro. The fusion was quantitated by the formation of a complex between avidin and biotHRP, originally internalized by fluid phase endocytosis respectively in acceptor and donor cells.

The experimental protocol is outlined in Fig. 6. Cells with implanted G were incubated at 37°C in the presence of 3.0 mg/ml avidin to cointernalize avidin with the G protein. At various times, the cells were returned to ice temperature and homogenized, and a PNS was prepared. The endocytic vesicles containing the G protein and avidin were then immunoisolated from the PNS onto a magnetic solid support using a mAb against G cytoplasmic domain (Gruenberg and Howell, 1986; Howell et al., 1989). The immunoisolated fractions provided the acceptor component in the cell-free fusion experiments. This protocol offers the advantage that the vesicles are bound to a solid support and therefore can be introduced into, and retrieved from, the reaction mixtures of the assay. In the assay, the immunoisolated acceptor was mixed with a donor PNS prepared from cells lacking the G protein that had internalized biotHRP for different times at 37°C. Fusion delivered biotHRP into the lumen of acceptor vesicles containing avidin. At the end of the incubation, the vesicles bound to the solid support were retrieved, washed,

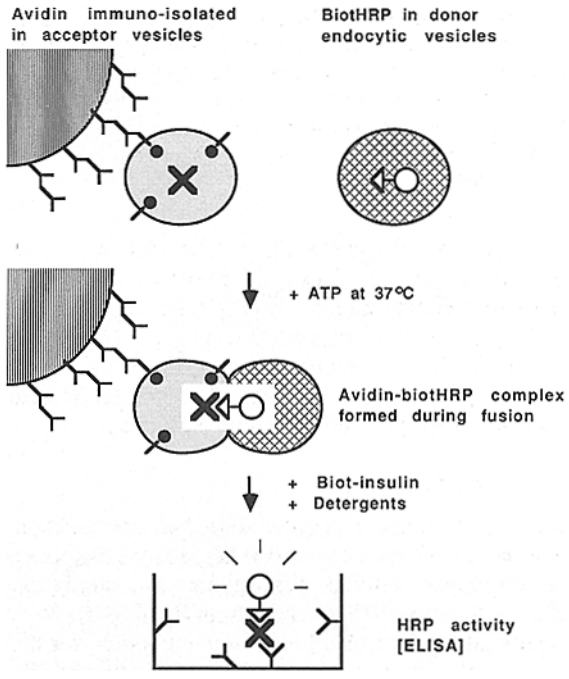

Figure 6. Outline of the cell-free assay.

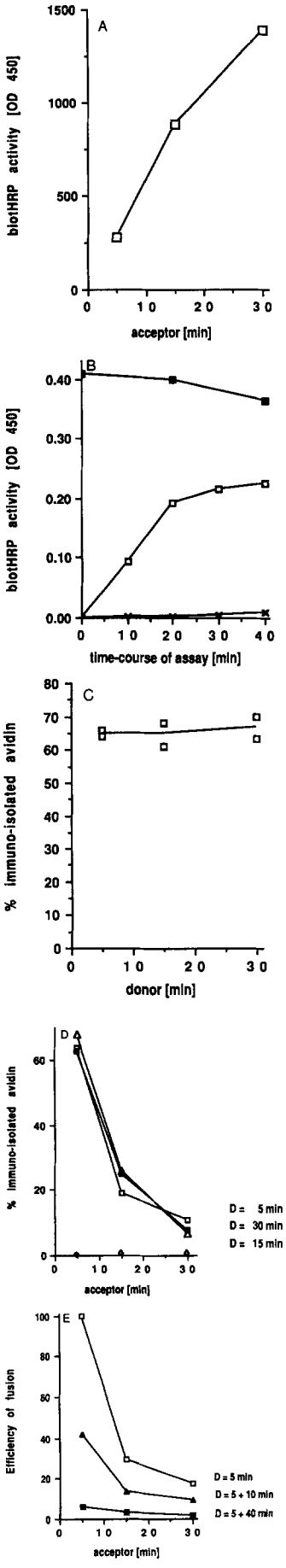

Figure 7. Cell-free fusion assay: the acceptor and the donor. (*A*) Avidin at 3 mg/ml (45.6 μM) was cointernalized with the G protein for 5, 15, and 30 min. The corresponding acceptor fractions were immunoisolated, incubated for 40 min at 37°C, under the same conditions as in the assay, and solubilized in the presence of exogenous biotHRP, omitting biotinylated insulin. The total amount of immunoisolated avidin present in the acceptor fractions was quantitated with the ELISA. (*B*) An immunoisolated acceptor fraction was prepared 5 min after internalization of 45.6 μM avidin, as in *A*. The donor was prepared after internalization of 1.7 mg/ml biotHRP for 30 min, which corresponds to the same molar concentration as avidin. The assay was carried out for the indicated times by mixing the acceptor and the donor at 37°C in the presence of an ATP-regenerating system (□). When an ATP-depleting system was used, or when the assay was carried out at 4°C, the signal was abolished (X). The fusion events were quantitated by the amount of avidin-biotHRP complex formed during the fusion using an ELISA. These values are compared with the total amount of avidin present in the acceptor during the assay (■). After 40 min, the avidin that has formed the fusion-specific complex with biotHRP (□) accounts for 65% of the avidin present in the acceptor (■). (*C*) The assay was carried out as in *B* with donors prepared after the indicated times of biotHRP internalization. (*D*) The acceptors were prepared after the indicated times of internalization and biotHRP was internalized in the donors for 5 (□), 15 (△), and 30 min (■). (*E*) The acceptor was prepared after 5 min internalization, as in *A*. BiotHRP was internalized in the donor cells for 5 min (□) or subsequently chased for 10 min (▲) and 40 min (■) in biotHRP-free medium. The values are expressed in percentage of the maximum efficiency at 5 min. The total amount of biotHRP present in the donor fractions decreased with the time of chase, due to recycling of the fluid phase (see Besterman et al., 1981). After 10 and 40 min chase, the donors contained, respectively, 72 and 58% of the biotHRP present in the 5-min donor. These values do not account for the decreased signal of fusion activity after chase.

and solubilized in detergent in the presence of biotinylated insulin to quench the unreacted avidin. Then, the fusion-specific complex was bound to a microtiter well via a polyclonal antibody against avidin and the HRP activity of the complex was quantified.

The assay relies on the quantification of avidin complexed to biotHRP during fusion. Therefore, it was important to establish first that the amount of avidin present in the acceptor fraction could be determined with the ELISA. These preliminary experiments were carried out as described above, except that the donor was omitted and an excess exogenous biotHRP replaced the biotinylated insulin during the detergent solubilization. With this protocol, the molecules of avidin immunosiolated in the acceptor fraction could be complexed with biotHRP. Fig. 7 *A* shows that an acceptor fraction immunoisolated 30 min after G protein/avidin cointernalization contained approximately five times more avidin than after 5 min. This accumulation of a fluid phase marker agreed well with the rate of HRP internalization in the cells during the same time course (Fig. 5 *C*) and subsequently immunoisolated (Gruenberg and Howell, 1987). With all acceptor fractions, the yield of immunoisolation from the PNS was ≈70% (not shown), as reported previously with HRP (Gruenberg and Howell, 1986). These experiments showed that (*a*) the amount of avidin-biotHRP complex could be quantified with the ELISA and (*b*) the immunoisolated acceptors remained intact during the different steps of the experiment (see also Fig. 8). The total amount of immunoisolated avidin was determined for each in vitro experiment and the value was used to calculate the efficiency of fusion (see below).

Early Endosome: Fusion Activity of the Acceptor

In a first series of experiments, the efficiency of fusion of the early endosomal vesicles immunoisolated 5 min after G protein internalization was determined (Fig. 7 *B*). The donor was prepared after continuous biotHRP internalization for 30 min. The time course of the fusion reaction itself is shown in Fig. 7B, in the presence (*open symbols*) and in the absence of ATP (*crosses*). The data confirmed that fusion is ATP dependent and blocked at 4°C, in agreement with our earlier studies (Gruenberg and Howell, 1986; 1987) and others (Davey et al., 1985; Braell, 1987; Diaz et al., 1988: Woodman and Warren, 1988). The total amount of avidin present in the acceptor fraction, assayed as in Fig. 7 *A*, remained constant after different times of in vitro incubation (Fig. 7 *B*, *solid symbols*) and when ATP was omitted (not shown). The efficiency of vesicle fusion was calculated as the fraction of the total immunoisolated avidin that formed the complex with biotHRP during the fusion reaction:

$$\text{avidin-biotHRP}_{\text{fusion + ATP}}/\text{avidin-biotHRP}_{\text{total}} \times 10^2.$$

The efficiency was 65% for an acceptor prepared 5 min after G protein/avidin cointernalization and a donor prepared after biotHRP continuous internalization for 30 min (Fig. 7 *B*). These data show that the early endosome exhibits a high fusion activity in vitro.

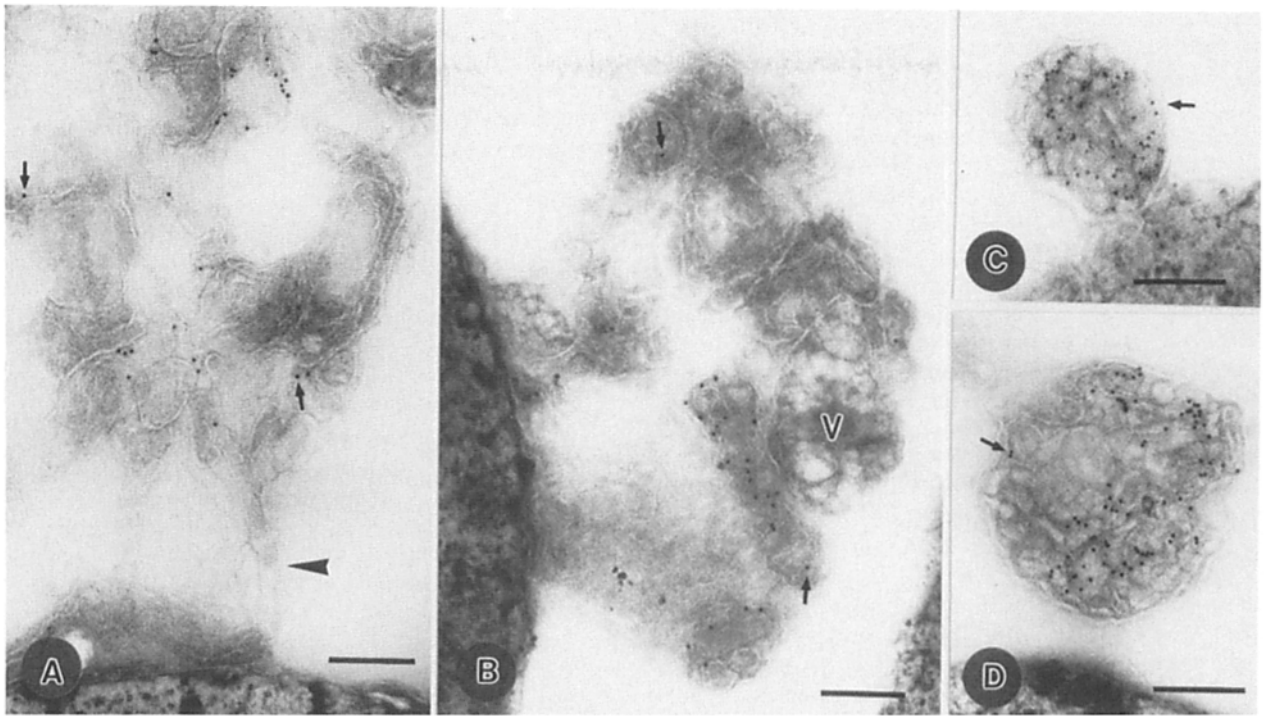

Figure 8. Morphology of early endosomal elements and spherical vesicles after immunoisolation. (*A* and *B*) The G protein was implanted and labeled with colloidal gold as in Fig. 1. After 5 min internalization, the early endosomal fraction was immunoisolated and prepared for electron microscopy using cryosections to visualize the membrane organization. Small arrows point at gold particles. In *A*, a tubule (*arrowhead*) connected to the immunoisolated structure is bound to the solid support; in *B*, the vesicular portion (*V*) of a tubulovesicular element can be visualized. (*C* and *D*) The experiment was as in *A*, except that internalization was for 45 min in the presence of 10 μM nocodazole. Under these conditions, the G protein/gold complexes did not reach acid phosphatase–positive structures and remained in large spherical vesicles (see Fig. 3). These vesicles were immunoisolated on the solid support. Bars, 0.2 μm.

Early Endosome: The Donor

In the experiments described above, the donor was prepared after continuous biotHRP internalization for 30 min and therefore could potentially provide partner vesicles from any stage of the endocytic pathway. To identify these partner vesicles, donor fractions were prepared after continuous internalization of biotHRP for 5, 15, and 30 min. Each donor was assayed with the early acceptor prepared after 5 min (Fig. 7 *C*). The fusion efficiency was already 65% with a donor prepared after 5 min internalization and remained at the same level with donors prepared after longer times of continuous internalization. This suggests that only the early endosomal vesicles of the donor fractions, corresponding to the internalization of biotHRP for 5 min, participate in the fusion with the early acceptor, also prepared after 5 min.

Next, the reciprocal experiment was carried out. The fusion efficiency was determined with acceptors immunoisolated after cointernalization of G protein/avidin for 5, 15, and 30 min. Each acceptor was then tested with donors prepared after 5, 15, and 30 min biotHRP internalization (Fig. 7 *D*). The fusion efficiency of the acceptors decreased with the time of G protein/avidin cointernalization and the kinetics of this decrease were essentially identical with the different donors. This decrease follows kinetics similar to those previously reported using a fusion-specific iodination of the G protein with a donor prepared after 30 min (Gruenberg and Howell, 1987). This experiment shows that only the early endosomal elements of both the acceptor and the donor exhibit a high fusion activity in the assay.

Finally, a pulse-chase protocol was used to confirm that only the early vesicles of the donor provided the fusion partners to the acceptor vesicles in the assay. The same experiment as in Fig. 7 *D* was repeated using donor fractions prepared after biotHRP internalization for 5 min, followed by incubations for 0, 10, and 40 min in biotHRP-free medium to chase the biotHRP to later stages of the pathway (Fig. 7 *E*). The data are expressed as a percentage of the maximum efficiency, which we define as that obtained after 5 min internalization. The 10-min chase decreased the efficiency to 40% of the value obtained with a 5-min pulse and the 40-min chase abolished the signal.

Chasing the Markers from the Early, Fusion-active Endosome Does Not Require Intact Microtubules

The in vitro experiments showed that fusion activity was at a maximum when the markers distributed in the early, tubulovesicular endosome and then decreased as the markers were chased from the early endosome to later stages of the pathway. Our in vivo data showed that in the absence of microtubules, the G molecules were endocytosed and sequentially appeared in the early endosome and then in the spherical, acid phosphatase–negative vesicles where they remained. Therefore, we asked whether the markers could be

chased out of the early, fusion-active endosome after microtubule depolymerization in our cell-free assay.

First, we investigated whether the early, fusion-active endosomal elements and the spherical vesicles containing the G molecules after nocodazole treatment retained their structure after immunoisolation (Fig. 8). In these experiments, the implanted G molecules were labeled with colloidal gold before internalization, as in Figs. 1–3. In a number of different cell types, the spherical vesicles contain a complex system of internal membranes that are clearly visualized in cryosections but poorly in conventional plastic sections (G. Griffiths, upublished observation). To visualize more clearly the internal structure and the membrane organization of the vesicle in this study, the samples were processed for cryosectioning. After 5 min internalization, tubular and tubulovesicular elements were observed that retained some structural features that were observed in the cell (compare Fig. 8, *A* and *B* with Fig. 1). These structures appeared similar to those revealed by a direct examination of the fusion product embedded in plastic (Gruenberg and Howell, 1987). Smaller tubules and vesicles were also immunoisolated (not shown; see Gruenberg and Howell, 1988). After 45 min, the immunoisolated fraction consisted of large spheres of ≈0.5 μm diameter containing the gold particles (compare Fig. 8, *C* and *D* with Fig. 2 *A* and Fig. 3). It is evident that these vesicles contain a complex organization of internal membranes also labeled with gold particles. A similar luminal organization was also observed in vesicular regions of early endosomal elements (see Fig. 8 *B*), suggesting that the spherical vesicles originate from the early endosome.

The cell-free assay was then used to determine whether the G molecules were chased from the early, fusion-active endosome in the absence of microtubules. When the transport of G molecules to acid phosphatase–positive prelysosomes was impaired in acceptor cells using nocodazole, the fusion activity of the different acceptor fractions remained as with fractions prepared from control cells (Fig. 9 *A*). The donors were prepared from cells containing intact microtubules after continuous internalization of biotHRP for 30 min to guarantee the detection of all fusion events that might occur in the assay.

Finally, we tested whether the fluid content, monitored with biotHRP, could also be chased from the early donor endosome when the microtubules were depolymerized. For this experiment, the donor fractions were prepared from cells with depolymerized microtubules, whereas the acceptor fractions were prepared from control cells (Fig. 9 *B*). A donor prepared 15 min after internalization in nocodazole-treated cells supported the fusion with the different acceptors as a control donor. However, when biotHRP was internalized for 15 min and subsequently chased for 30 min, the signal was abolished. These experiments demonstrate that both the endosomal content and the membrane-spanning G protein are chased from the early, fusion active endosome in the absence of microtubules.

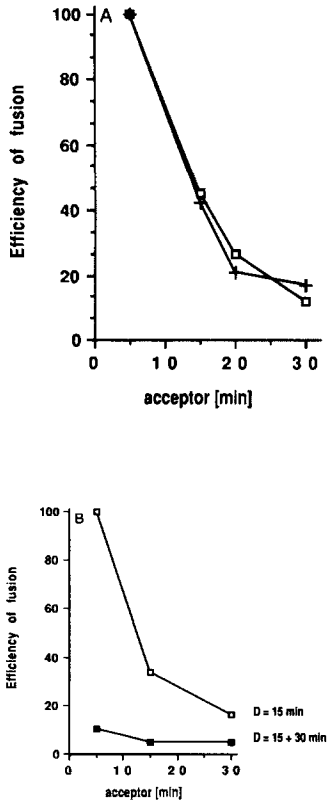

Figure 9. Cell-free fusion assay: acceptor (*A*) or donor (*B*) prepared after microtubule depolymerization. (*A*) Cells with implanted G protein were incubated in the presence of avidin for the indicated times with (X) or without (□) nocodazole. Acceptor fractions were immunoisolated from these cells after the indicated times and used in the cell-free assay as in Fig. 7 *B*. The donor fraction was prepared after 30 min biotHRP internalization in the absence of nocodazole. The fusion efficiency is expressed as in Fig. 7 *E*. (*B*) The acceptor fractions were prepared as in *A*, in the absence of nocodazole. The donors were prepared from cells treated with 10 μM nocodazole after internalization of biotHRP for 15 min (□) followed by a 30-min chase in biotHRP-free medium (■). After 30 min chase, the donor contained 65% of the biotHRP present in the 15-min pulse (see Fig. 7).

Discussion

In this paper we have dissected the early stage of membrane traffic in endocytosis both in vivo and in vitro. For these studies, the *trans*-membrane glycoprotein G was implanted into the plasma membrane and subsequently endocytosed for different times at 37°C. Because the G molecules were internalized as a synchronous wave, they provided both a morphological and a biochemical marker of the pathway and a cytoplasmic epitope for the immunoisolation of the corresponding endosomal fractions. After cointernalization of the G protein with avidin, the immunoisolated fractions were used as acceptors in a cell-free assay that measured their fusion activity with donor fractions prepared from cells that had internalized biotHRP. With this approach, two different endosomal structures were identified, fractionated, and functionally characterized: the early endosomal compartment and the putative carrier vesicles, involved in the transport between the early endosome and a later stage of the pathway, presumably the prelysosome (or late endosome).

After 5 min internalization at 37°C, 65% of the G molecules are internalized into early endosomal elements. At the morphological level, these separate elements form a network of tubular, cisternal and tubulovesicular structures. We define these elements as the first station in the pathway where internalized molecules are routed to their cellular destinations. After longer incubations at 37°C, the G molecules internalized into the early endosome are either recycled back to the cell surface or chased to a later stage of the pathway with similar kinetics ($t_{1/2} \approx 5$ min). This agrees well with a consensus emerging from several studies that the rapid recycling of internalized receptors back to the plasma membrane occurs from an early endosome (Ciechanover et al., 1983; Geuze et al., 1983; Harding et al., 1983; Hopkins and Trowbridge, 1983; Oka and Weigel, 1983*b*; Mellman et al., 1984; Mueller and Hubbard, 1986).

The fusion activity in vitro of an acceptor fraction immunoisolated after 5 min internalization was high and cor-

responded to a mixing of 65% of its luminal content with donor vesicles. This high value suggests that the fusion active vesicles represent a major population of the vesicles in the acceptor fraction. Because the majority of the G molecules reside in the early, tubulovesicular endosome after 5 min internalization, the vesicles active in the assay must correspond to elements of the early endosome. This confirms our earlier observations obtained by direct morphological examination of the fusion product (Gruenberg and Howell, 1986). Characterization of the donor in the fusion reaction showed that the high fusion activity is supported only by endocytic vesicles prepared 5 min after internalization of biotHRP. Fusion activity decreased when either marker, the membrane-spanning protein G in the acceptor or the endosomal content in the donor, were transported to a later stage of the pathway in vivo, before preparation of the fractions. This reduced activity cannot be explained simply by an inactivation of the fraction after immobilization on the solid support. Loss of activity of the fusion active acceptor was not observed during the time course of our in vitro assay. The results also indicated that the decreased activity of later acceptors was not due to a failure to immunoisolate later endosomes nor due to a decrease in latency. It remains to be established whether relatively little membrane fusion actually occurs at later stages of the pathway in the cell or whether these fusions have other requirements that are not fulfilled by our present in vitro conditions.

A possible interpretation of our observations is that the donor vesicles in the assay are incoming vesicles that deliver their cargo by fusion to the first station of the pathway, the immunoisolated acceptor. However, the total number of incoming vesicles present at any time point represent a small fraction of the total volume of the early endosomal, (≈7%; Griffiths, G., R. Back, and M. Marsh, manuscript in preparation). It seems unlikely that these vesicles could support the high efficiency of fusion we observe. This high efficiency suggests that the fusion-active vesicles in the donor PNS are also elements of the early endosome that fuse with the early acceptor or that both are connected by vesicular traffic. If these in vitro findings can be extrapolated to the in vivo functions, it suggests that the individual elements of the early endosome, rather than being separate functional units, actively interact with each other, thereby exchanging membrane and content.

Our results show another striking difference between early and late endosomes, namely that all the functions of the early endosome we have measured do not require intact microtubules, in contrast to later stages. After depolymerization, both the rates and the amount of internalization and recycling remained identical to that seen in the control cells. Our cell-free data also indicated that the membrane-spanning G protein (acceptor) and the endosomal content (donor) were transported in the absence of microtubules from the fusion-active, early endosome to a more distal endocytic compartment. Transport of the endosomal content beyond the early endosome in the presence of nocodazole was also shown by our in vivo observation that HRP internalization did not reach an early plateau but continued to accumulate in the cells with increasing times of incubation. That the G molecules were chased from the early endosome after microtubule depolymerization, was also confirmed by the morphometric analysis of G protein subcellular distribution.

When the microtubules were depolymerized, transport of the G molecules to prelysosomes and lysosomes was significantly reduced, even after 45 min. The G molecules were then observed in spherical, acid phosphatase-negative vesicles (0.4–0.7 μm). In vitro these vesicles exhibit little, if any, fusion activity with elements of the early endosome or with each other. They are clearly distinct from the early, tubulovesicular elements and from the prelysosomes (or late endosomes) with a complex multi-vesicular appearance (for a morphological description, see for example Wall et al., 1980; Hopkins, 1983; Griffiths et al., 1988). Griffiths et al. (1988) have observed spherical vesicles proximal to the block of endocytosis at 20°C, which have the same morphological appearance as the spherical vesicles described here, whereas prelysosomes were distal to the block. We also observed these spherical vesicles in control cells between 5 and 15 min internalization, when the G molecules were transported from the early, tubulovesicular endosome to the acid phosphatase-positive prelysosomes.

Two models have been proposed for membrane traffic in endocytosis (reviewed and summarized by Helenius et al., 1983). The first model predicts that early endosomal elements undergo a maturation process and become late endosomes, whereas the second model predicts that early and late endosomes are preexisting compartments connected by vesicular traffic. Definite evidence supporting either model remains to be obtained. However, the observed fusion specificity of early endosomal elements must clearly reflect the presence of unique molecules in their membranes. This is also supported by the recent observations of Schmid et al. (1988) that different proteins are iodinated in an early and a late endosomal fraction. In both our and their studies, the early endosome is likely to encompass the same compartment; in their studies, the early endosome contains both lactoperoxidase internalized for 4 min and transferrin, which recycles to the cell surface with kinetics similar to the G protein (Hopkins and Trowbridge, 1983). It is more difficult to ascertain clearly whether the late transferrin-negative endosome of Schmid et al. (1988), prepared after 15 min lactoperoxidase internalization, corresponds to the spherical vesicles, to the prelysosomes, or to a mixture of both. In any case, we believe that both the presence of distinct molecules in the studies of Schmid et al. (1988) and the high, specific fusion activity we observe, argue in favor of a preexisting, early endosomal compartment. We suggest that the decrease in fusion activity after 5 min internalization measures the export of the G molecules from the early fusion-active endosome to distinct vesicles with little fusion activity in our assay. Our data show that these vesicles correspond to the large, spherical vesicles in which the G molecules appear after leaving the early endosome but before reaching the prelysosomes.

We propose that a relatively high number of small incoming vesicles deliver their membrane and content from the plasma membrane to the early endosome and that a low number of large, spherical carrier vesicles then collect the material destined to degradation. Because early endosomal elements may interact with each other by fusion or vesicular traffic, a carrier vesicle could conceivably pool this material from more than one element. A single large carrier of diameter ≈0.5 μm could accommodate the volume of fluid endocytosed by ≈100 coated vesicles (diameter = 0.1 μm), and

thus permit a more efficient packaging of the solutes destined to degradation. These calculations take into account an estimated 50% recycling of the endosomal content from the early endosome (Besterman et al., 1981; Adams et al., 1982). Our data leads us to suggest that these carrier vesicles are generated at the first endosomal station and subsequently transport the materials destined to be degraded to the prelysosome. This process is microtubule dependent, suggesting that the carrier vesicles interact specifically with the microtubules (see below). The carrier vesicles may in fact correspond to the endocytic vesicles shown to move in vivo between the periphery and the center of the cell (Herman and Albertini, 1984; Matteoni and Kreis, 1987; De Brabander et al., 1988). The relatively slow rate of this process (5–15 min) and the large size of the vesicles could explain why the in vivo movement of distinct vesicles has been easier to visualize in endocytosis than in other pathways of membrane traffic.

After 15 min internalization, the G molecules have appeared in acid phosphatase–positive prelysosomes, which are often observed in the perinuclear region, and, after 30–45 min, degradation of the G molecules to a 28-kD peptide occurs. The precise sequence of events leading to delivery to prelysosomes or lysosomes are not clear. After 30 min, the fusion activities of both the donor and the acceptor have dropped to ≈10% of the value at 5 min. This is unlikely to reflect a deterioration of the late acceptor fractions during immunoisolation because they remained latent and since the same low fusion activity was also observed with donor fractions, which were not immunoisolated, after chasing a pulse of biotHRP to late stages of the pathway. This reduced efficiency agrees well with recent in vivo observations of De Brabander et al. (1988), who have shown that endocytic vesicles move back and forth in a microtubule-dependent manner between the plasma membrane and the perinuclear region, where the internalized probe eventually accumulates after 15–30 min. It is tempting to propose that microtubules increase the frequency of encounters between carrier vesicles and pre-lysosomes in the perinuclear region, thereby increasing the efficiency of an otherwise inefficient delivery process. In any case, these late endocytic events are clearly very distinct from the rapid internalization into, and recycling and export from, the early endosome.

The late acid phosphatase–positive endosome (prelysosome), where the G molecules are observed before being delivered to the lysosomes, remains to be characterized. Griffiths et al. (1988) have recently described a prelysosomal compartment situated close to, but functionally distinct from, the *trans*-Golgi network, in normal rat kidney cells. These authors have shown that this compartment accumulates the cation-independent mannose-6-phosphate receptor (MPR), whereas the lysosomes are MPR negative (Sahagian and Neufeld, 1983; Geuze et al., 1985; Brown et al., 1986). This compartment labels with both antibodies to lysosomal enzymes and to Igp120, an antigen purified from lysosomal membranes (Lewis et al., 1985). Recent data indicate that it also reacts cytochemically for acid phosphatase (Griffiths, G., R. Matteoni, R. Back and B. Hoflack, manuscript in preparation). This prelysosomal compartment is postulated to be the last endosomal station before the lysosomes where newly synthesized lysosomal hydrolases are delivered from the *trans*-Golgi network. At present we are unable to identify this compartment in BHK cells, because our antibody against the MPR reacts poorly with BHK cells. However, parallel studies with the NRK cell indicate that a significant amount of G molecules has reached this MPR-rich compartment after 20 min internalization (unpublished data). This observation and the typical morphology of the MPR-rich compartment lead us to believe that the acid phosphatase–positive prelysosome in BHK cells corresponds to a structure similar to the MPR-rich compartment described in NRK cells.

Small amounts of hydrolases have been also detected in the early endosome (Diment and Stahl, 1985; Roederer et al., 1987). This may explain our observation that a small fraction of the G protein is first cleaved to a membrane-spanning 60-kD polypeptide, even in the absence of intact microtubules. The second cleavage of the G protein to a 28-kD peptide clearly occurs after the microtubule-dependent step of the pathway, as this process is inhibited after depolymerization. Whether this processing occurs in the prelysosomes or in the lysosomes remains to be established. Clearly, the observation that little labeled G protein is degraded beyond the 28-kD peptide during the time course of these experiments suggests that this process might in fact be initiated in the former compartment.

We conclude that early endocytosis proceeds in at least two discrete steps. First, internalized molecules are delivered to the early endosomal compartment, where they are routed to be recycled or transported to a later stage. These functions do not require an intact microtubule network. The elements of this first station of endocytosis exhibit a high and specific fusion activity with each other, suggesting that in vivo, they are not functionally independent but, rather, exchange their membrane and content. Subsequently, a slower microtubule-dependent process mediates the transport of large vesicles from the early endosome to a late, acid phosphatase–positive endosome (prelysosome). The fusion activity with other endocytic vesicles is significantly reduced during this transport. It is now a major challenge to identify the molecular components that provide the high activity and specificity of fusion to the early endosome, as well as those that may mediate the binding of vesicles to microtubules.

We wish to thank Ruth Back for excellent technical assistance in electron microscopy. We also thank Eileen Devaney, Steven Fuller, Bernard Hoflack, Thomas Kreis, Paul Luzio, Kai Simons, and John Tooze for critically reading the manuscript. We thank John Ugelstad and Ruth Schmid for providing us with the magnetic solid supports (now available from Dynal, A. S.; Oslo and Great Neck, NY). We also wish to thank E. Soini and I. Hemmilä for their help in setting up the time-resolved fluorescence assay and for the labeling with Europium. J. Gruenberg was supported by a fellowship from the Swiss National Science Foundation.

Received for publication 12 July 1988, and in revised form 28 December 1988.

References

Adams, C. J., K. M. Maurey, and B. Storrie. 1982. Exocytosis of pinocytic contents by Chinese hamster ovary cells. *J. Cell Biol.* 93:632–637.

Altstiel, L., and D. Branton. 1983. Fusion of coated vesicles with lysosomes: measurement with a fluorescent assay. *Cell.* 32:921–929.

Baenziger, J., and D. Fiete. 1986. Separation of two populations of endocytic vesicles involved in receptor-ligand sorting in rat hepatocytes. *J. Biol. Chem.* 261:7445–7454.

Balch, W. E., W. G. Dunphy, W. A. Braell, and J. E. Rothman. 1984. Reconstitution of the transport of protein between successive compartments of the Golgi measured by the coupled incorporation of N-acetylglucosamine. *Cell.* 39:405–416.

Berg, T., G. M. Kindberg, T. Ford, and R. Blomhoff. 1985. Intracellular transport of asialoglycoproteins in rat hepatocytes. Evidence for two sub-

populatioms of lysosomes. *Exp. Cell Res.* 161:285–296.
Besterman, J. M., J. A. Airhart, R. C. Woodworth, and R. B. Low. 1981. Exocytosis of pinocytosed fluid in cultured cells: kinetic evidence for rapid turnover and compartmentation. *J. Cell Biol.* 91:716–727.
Bordier, C. 1981. Phase separation of integral membrane proteins in Triton X-114 solution. *J. Biol. Chem.* 256:1604–1607.
Bradford, M. M. 1976. A rapid and sensitive method for the quantitation of microgram quantities of protein utilizing the principle of protein-dye binding. *Anal. Biochem.* 72:248–254.
Braell, W. A. 1987. Fusion between endocytic vesicles in a cell-free system. *Proc. Natl. Acad. Sci. USA.* 84:1137–1141.
Branch, W. J., B. M. Mullock, and J. P. Luzio. 1987. Rapid subcellular fractionation of the rat liver endocytic compartments involved in transcytosis of polymeric immunoglobulin A and endocytosis of asialofetuin. *Biochem. J.* 244:311–315.
Brown, W. J., J. Goodhouse, and M. G. Farquhar. 1986. Mannose-6-phosphate receptors for lysosomal enzymes cycle between the Golgi complex and endosomes. *J. Cell Biol.* 10:1235–1247.
Caron, J. M., A. L. Jones, and M. W. Kirschner. 1985. Autoregulation of tubulin synthesis in hepatocytes and fibroblasts. *J. Cell Biol.* 101:1763–1772.
Ciechanover, A., A. L. Schwartz, and H. F. Lodish. 1983. The asialoglycoprotein receptor internalizes and recycles independently of the transferrin and insulin receptors. *Cell.* 32:267–275.
Davey, J., S. M. Hurtley, and G. Warren. 1985. Reconstitution of an endocytic fusion event in a cell-free system. *Cell.* 43:643–652.
De Brabander, M., R. Nuydens, H. Geerts, and C. R. Hopkins. 1988. Dynamic behaviour of the transferrin receptor followed in living epidermoid carcinoma (A431) cells with nanovid microscopy. *Cell Motil. Cytoskeleton.* 9:30–47.
Diaz, R., L. Mayorga, and P. Stahl. 1988. In vitro fusion of endosomes following receptor-mediated endocytosis. *J. Biol. Chem.* 263:6093–6100.
Diment, S., and P. Stahl. 1985. Macrophage endosomes contain proteases which degrade endocytosed protein ligands. *J. Biol. Chem.* 260:15311–15317.
Fuchs, R., S. Schmid, and I. Mellman. 1989. A possible role for sodium potassium-ATPase in regulating ATP-dependent endosome acidification. *Proc. Natl. Acad. Sci. USA.* 86:539–543.
Geuze, H. J., J. W. Slot, G. J. A. M. Strous, A. Hasilik, and K. von Figura. 1985. Possible pathways for lysosomal enzyme delivery. *J. Cell Biol.* 101:2253–2262.
Geuze, H. J., J. W. Slot, G. J. A. M. Strous, H. F. Lodish, and A. L. Schwartz. 1983. Intracellular site of asialoglycoprotein receptor-ligand uncoupling: double-label immuno-electron microscopy during receptor-mediated endocytosis. *Cell.* 32:277–287.
Goldstein, J. L., M. S. Brown, R. G. W. Anderson, D. W. Russel, and W. J. Schneider. 1985. Receptor-mediated endocytosis: concepts emerging from the LDL receptor system. *Annu. Rev. Cell Biol.* 1:1–39.
Griffiths, G., and H. Hoppeler. 1986. Quantitation of immunocytochemistry: correlation of immunogold labeling to absolute number of membrane antigens. *J. Histochem. Cytochem.* 34:1389–1398.
Griffiths, G., B. Hoflack, K. Simons, I. Mellman, and S. Kornfeld. 1988. The mannose-6-phosphate receptor and the biogenesis of lysosomes. *Cell.* 52: 329–341.
Griffiths, G., P. Quinn, and G. Warren. 1983*a*. Dissection of the Golgi complex. I. Monensin inhibits the transport of viral proteins from *medial* to *trans* Golgi cisternae in baby hamster kidney cells infected with Semliki Forest virus. *J. Cell Biol.* 96:835–850.
Griffiths, G., K. Simons, G. Warren, and K. T. Tokuyasu. 1983*b*. Immunoelectron microscopy using thin, frozen sections: applications to studies of the intracellular transport of Semliki Forest virus spike glycoproteins. *Methods Enzymol.* 96:435–450.
Gruenberg, J., and K. E. Howell. 1985. Immuno-isolation of vesicles using antigenic sites either located on the cytoplasmic or the exoplasmic domain of an implanted viral protein. A quantitative analysis. *Eur. J. Cell Biol.* 38: 312–321.
Gruenberg, J., and K. E. Howell. 1986. Reconstitution of vesicle fusions occurring in endocytosis with a cell-free system. 1986. *EMBO (Eur. Mol. Biol. Organ.) J.* 5:3091–3101.
Gruenberg, J., and K. E. Howell. 1987. An internalized transmembrane protein resides in a fusion-competent endosome for less than 5 minutes. *Proc. Natl. Acad. Sci. USA.* 84:5758–5762.
Gruenberg, J., and K. E. Howell. 1988. Fusion in the endocytic pathway reconstituted in a cell-free system using immuno-isolated fractions. *In* Cell-free Analysis of Membrane Traffic. D. J. Morré, K. E. Howell, G. M. W. Cook, and W. H. Evans, editors. Alan R. Liss, Inc., New York. 317–332.
Harding, C., J. Heuser, and P. Stahl. 1983. Receptor-mediated endocytosis of transferrin and recycling of the transferrin receptor in rat reticulocytes. *J. Cell Biol.* 97:329–339.
Helenius, A., I. Mellman, D. Wall, and A. Hubbard. 1983. Endosomes. *Trends Biochem. Sci.* 8:245–250.
Hemmilä, I., S. Dakubu, V.-M. Mukkala, H. Siitari, and T. Lövgren. 1984. Europium as a label in time-resolved immunofluorometric assays. *Anal. Biochem.* 137:335–343.
Herman, B., and D. F. Albertini. 1984. A time-lapse video image intensification analysis of cytoplasmic organelle movements during endosome translocation. *J. Cell Biol.* 98:565–576.
Hirsch, J. G. 1962. Cinemicrographic observations on granule lysis in polymorphonuclear leucocytes during phagocytosis. *J. Exp. Med.* 116:827–833.
Hopkins, C. R. 1983. The importance of the endosome in the intracellular traffic. *Nature (Lond.).* 305:684–685.
Hopkins, C. R., and I. S. Trowbridge. 1983. Internalization and processing of transferrin and the transferrin receptor in human carcinoma A 431 cells. *J. Cell Biol.* 97:508–521.
Howell, K. E., W. Ansorge, and J. Gruenberg. 1988*a*. Magnetic free flow immuno-isolation system designed for sub-cellular fractionation. *In* Microspheres: Medical and Biological Applications. A. Rembaum, and Z. Tokes editors. CRC Press, Boca Raton, FL. 33–52.
Howell, K. E., J. Gruenberg, I. Ito, and G. E. Palade. 1988*b*. Immuno-isolation of sub-cellular components. *In* Cell-free Analysis of Membrane Traffic. D. J. Morré, K. E. Howell, G. M. W. Cook, and W. H. Evans, editors. Alan R. Liss, Inc., New York. 77–90.
Howell, K. E., R. Schmid, J. Ugelstad, and J. Gruenberg. 1989. Immunoisolation using magnetic solid supports: subcellular fractionation for cell-free functional studies. *Methods Cell Biol.* In press.
Kreis, T. E. 1986. Microinjected antibodies against the cytoplasmic domain of vesicular stomatitis virus glycoprotein block its transport to the cell surface. *EMBO (Eur. Mol. Biol. Organ.) J.* 5:931–941.
Lewis, V., J. A. Green, M. Marsh, P. Vihko, A. Helenius, and I. Mellman. 1985. Glycoproteins of the lysosomal membrane. *J. Cell Biol.* 100:1839–1847.
Limet, J. N., J. Quintart, Y.-J. Schneider, and P. J. Courtoy. 1985. Receptor-mediated endocytosis of polymeric IgA and galactosylated serum albumin in rat liver. *Eur. J. Biochem.* 146:539–548.
Maizel, J. V., Jr. 1971. Polyacrylamide electrophoresis of viral proteins. *Methods Virol.* 5:179–246.
Marsh, M., G. Griffiths, G. E. Dean, I. Mellman, and A. Helenius. 1986. Three-dimensional structure of endosomes in BHK-21 cells. *Proc. Natl. Acad. Sci. USA.* 83:2899–2903.
Matteoni, R., and T. E. Kreis. 1987. Translocation and clustering of endosomes and lysosomes depend on microtubules. *J. Cell Biol.* 105:1253–1265.
Mellman, I., H. Plutner, and P. Ukkonen. 1984. Internalization and rapid recycling of macrophage Fc receptors tagged with monovalent antireceptor antibody: possible role of a prelysosomal compartment. *J. Cell Biol.* 98:1163–1169.
Mueller, S. C., and A. Hubbard. 1986. Receptor-mediated endocytosis of asialoglycoproteins by rat hepatocytes: receptor-positive and receptor-negative endosomes. *J. Cell Biol.* 102:932–942.
Oka, J. A., and P. H. Weigel. 1983*a*. Microtubule-depolymerizing agents inhibit asialo-orosomucoid delivery to lysosomes but not its endocytosis or degradation in isolated rat hepatocytes. *Biochim. Biophys. Acta.* 763:368–376.
Oka, J. A., and P. H. Weigel. 1983*b*. Recycling of the asialoglycoprotein receptor in isolated rat hepatocytes. Dissociation of internalized ligand from receptor occurs in two kinetically and thermally distinguishable compartments. *J. Biol. Chem.* 258:10253–10262.
Pastan, I. H., and W. C. Willingham. 1981. Journey to the center of the cell: role of the receptosome. *Science (Wash. DC).* 214:504–509.
Pastan, I. H., and W. C. Willingham, editors. 1985. Endocytosis. Plenum Publishing Corp., New York London. 326 pp.
Pearse, B. M. F. 1987. Clathrin and coated vesicles. *EMBO (Eur. Mol. Biol. Organ.) J.* 6:2507–2512.
Phaire-Washington, L., S. C. Silverstein, and E. Wang. 1980. Phorbol myristate acetate stimulates microtubule and 10-nm filament extension and lysosome redistribution in mouse macrophages. *J. Cell Biol.* 86:641–655.
Roederer, M., R. Bowser, and R. F. Murphy. 1987. Kinetics and temperature-dependence of exposure of endocytosed material to proteolytic enzyme and low pH: evidence for a maturation model for the formation of lysosomes. *J. Cell. Physiol.* 131:200–209.
Rose, J. K., and C. J. Gallione. 1981. Nucleotide sequence of the mRNA's encoding the vesicular stomatitis virus G and M proteins determined from cDNA clones containing the complete coding regions. *J. Virol.* 39:519–528.
Sahagian, G. G., and E. F. Neufeld. 1983. Biosynthesis and turnover of the mannose-6-phosphate receptor in cultured Chinese hamster ovary cells. *J. Biol. Chem.* 258:7121–7128.
Schmid, S. L., R. Fuchs, P. Male, and I. Mellman. 1988. Two distinct subpopulations of endosomes involved in membrane recycling and transport to the lysosomes. *Cell.* 52:73–83.
Silverstein, S. C., R. M. Steinman, and Z. A. Cohn. 1977. Endocytosis. *Annu. Rev. Biochem.* 46:669–672.
Soini, E., and I. Hemmilä. 1979. Fluoroimmunoassays: present status and key problems. *Clin. Chem.* 25:353–361.
Soini, E., and H. Kojola. 1983. Time-resolved fluorometer for lanthanide chelates—A new generation of nonisotopic immunoassays. *Clin. Chem.* 29: 65–68.
Steinman, R. M., I. S. Mellman, W. A. Muller, and Z. A. Cohn. 1983. Endocytosis and the recycling of plasma membrane. *J. Cell Biol.* 96:1–27.
Storrie, B., R. R. Pool Jr., M. Sachdeva, K. M. Maurey, and C. Oliver. 1984. Evidence for both prelysosomal and lysosomal intermediates in endocytic pathways. *J. Cell Biol.* 98:108–115.
Swanson, J., A. Bushnell, and S. C. Silverstein. 1987. Tubular lysosome mor-

phology and distribution within macrophages depend on the integrity of cytoplasmic microtubules. *Proc. Natl. Acad. Sci. USA.* 84:1921–1925.

Tran, D., J.-L. Carpentier, F. Sawano, P. Gorden, and L. Orci. 1987. Ligands internalized through coated or noncoated invaginations follow a common intracellular pathway. *Proc. Natl. Acad. Sci. USA.* 84:7957–7961.

Ugelstad, J., L. Söderberg, A. Berge, and J. Bergström. 1983. Monodisperse polymer particles—a step forward for chromatography. *Nature (Lond.).* 303:95–96.

Wall, D. A., G. Wilson, and A. L. Hubbard. 1980. The galactose-specific recognition system of mammalian liver: the route of ligand internalization in rat hepatocytes. *Cell.* 21:79–93.

Wall, D. A., and A. L. Hubbard. 1985. Receptor-mediated endocytosis of asialoglycoproteins by rat liver hepatocytes: biochemical characterization of the endosomal compartments. *J. Cell Biol.* 101:2104–2112.

Weibel, E. W. 1979. Stereological Methods: Practical Methods for Biological Morphometry. Vol. 1. Academic Press, New York. 415 pp.

White, J., J. Kartenbeck, and A. Helenius. 1980. Fusion of Semliki Forest virus with the plasma membrane can be induced by low pH. *J. Cell Biol.* 8:264–272.

Wileman, T., C. Harding, and P. Stahl. 1985. Receptor-mediated endocytosis. *Biochem. J.* 232:1–14.

Wolkoff, A. D., R. D. Klausner, G. Ashwell, and J. Harford. 1984. Intracellular segregation of asialoglycoproteins and their receptors: a prelysosomal event subsequent to dissociation of the ligand-receptor complex. *J. Cell Biol.* 98:375–381.

Woodman, P. G., and G. Warren. 1988. Fusion between vesicles from the pathway of receptor-mediated endocytosis in a cell-free system. *Eur. J. Biochem.* 173:101–108.